Designing artificial zinc phosphate tribofilms with tailored mechanical properties by altering the chain length

Sebastian Lellig [a,b,*], Subisha Balakumar [a], Peter Schweizer [b], Eva B. Mayer [a], Simon Evertz [a], Marcus Hans [a], Damian M. Holzapfel [a], Yin Du [c], Qing Zhou [c], Martin Dienwiebel [d], Johann Michler [b,e], Jochen M. Schneider [a,f]

[a] Materials Chemistry, RWTH Aachen University, Aachen, Germany
[b] Laboratory for Mechanics of Materials and Nanostructures, Empa, Swiss Federal Laboratories for Materials Science and Technology, Thun, Switzerland
[c] Research & Development Institute, Northwestern Polytechnical University in Shenzhen, Shenzhen City, 518063, PR China
[d] Institute for Applied Materials IAM-ZM, Karlsruhe Institute of Technology KIT, Karlsruhe, Germany
[e] EPFL - École polytechnique fédérale de Lausanne, Lausanne, Switzerland
[f] Max-Planck-Institute for Sustainable Materials GmbH, Department Structure and Nano-/ Micromechanics of Materials, Group Self-Reporting Materials, Düsseldorf, Germany

ARTICLE INFO

ABSTRACT

Zinc dialkyldithiophosphate (ZDDP), as the most prominent lubrication additive, forms tribofilms consisting primarily of zinc phosphate glasses containing sulfides. As sulfur is linked to environmental concerns, sulfur-free zinc phosphate coatings have been sputtered from a $Zn_3(PO_4)_2$ target and investigated here.

Based on the bridging to non-bridging oxygen ratio, determined by X-ray photoelectron spectroscopy (XPS), the as deposited coatings are classified as metaphosphates. As the annealing temperature is increased, the chain lengths are reduced, as witnessed by XPS data indicated by a loss of phosphorus and oxygen of the coating surface, likely due to hydrolysis with water from the atmosphere.

Transmission electron microscopy energy-dispersive X-ray spectroscopy line scans show that the XPS-revealed composition change of the coating surface upon annealing occurs over the whole thickness of the coating. This alteration in composition and chain length reductions causes a rise in hardness, reduced Young's modulus, and wear resistance. Therefore, the properties of the artificial zinc phosphate tribofilms can be tailored via a thermally stimulated composition change, causing an alternation in chain length from meta- to orthophosphate and thereby enabling the design of coatings with desired mechanical properties.

1. Introduction

Regarding the environmental challenges of current times, durability and long-lastingness have turned into focus. One of the most important fields is wear reduction leading to longer life-times of highly strained components. For that, thin films are used as protective coatings [1].

Zinc dialkyldithiophosphate (ZDDP) is one of the most prominent lubricant additives used for wear reduction [2–5]. Thereby, a tribofilm is formed under load by the agglomeration of distinct islands [6–8], which consists primarily of zinc phosphate glass protecting the underlying material [2,9]. Additionally, zinc phosphates can be used in a wide array of applications including photonics [10–12], corrosion resistance [13] and biomedical applications [14].

The zinc phosphate glasses formed by ZDDP are composed of a fundamental structure with a tetrahedral geometry, see Table 1. These orthophosphates possess a central phosphorus atom, which is surrounded by four oxygen atoms. To form longer phosphate chains, these blocks are linked via the P—O—P bond. For even longer chains, cross-linkage can occur as well [15,16]. Chains consisting only of the basic building block are called orthophosphates. If two of these blocks link via the bridging oxygen atom, pyrophosphates are formed. Longer chains are characterized as polyphosphates, whereby infinitely long chains are labeled as metaphosphates. Ultraphosphates (P_2O_5) are present once cross-linkage between these chains occurs [15–17].

The chain length can be estimated by the zinc to phosphorus Zn/P ratio as zinc functions as a glass modifier, breaking up the P=O bonds

---

Table 1

Characteristic BO/NBO ratios for different structures and chain lengths. Depictions of different chain types reconstructed after [17]. The blue, red, green, and purple dots indicate zinc, non-bridging oxygen, bridging oxygen, and phosphorus atoms, respectively.

Structure	Chemical formula [19]	Chain length	BO/NBO [16]
Orthophosphate	$Zn_3(PO_4)_2$	1	0
Pyrophosphate	$Zn_2P_3O_7$	2	1/6
Polyphosphate	–	>2	1/6 < x > 0.5
Metaphosphate	$Zn(PO_3)_2$	Infinite	0.5
Ultraphosphate	–	Cross-linked	>0.5
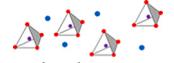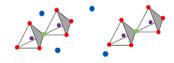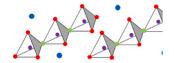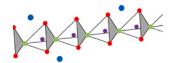
and forming P—O—Zn [18]. A lower Zn/P ratio indicates longer phosphate chains [17]. To quantify the specific chain length, the bridging (BO) to non-bridging oxygen (NBO) ratio is investigated. Hereby, the O 1s peak is split into two components, whereby the non-bridging oxygen peak is located at a binding energy 1.6 eV lower than the bridging oxygen peak. As bridging oxygen only occurs in the case that the basic building blocks are connected, the BO/NBO ratio is less dependent on the composition than the Zn/P ratio. An increase in the ratio thereby indicates an elongation of the chains [16,17]. Characteristic values for the BO/NBO ratios are shown in Table 1.

Protective thin films formed by ZDDP can be achieved in the form of thermal films, which form at elevated temperatures, or tribofilms, which are stable in an oil environment [20], forming under mechanical loads [2,21–23], which according to Zhang et al. is due to applied shear stresses [24]. Thereby, only in the rubbing tracks tribofilm formation can be observed, while in areas close to these tracks, the film growth is minimal [22]. While thermal films, which are formed at temperatures lower than 100 °C, consist mostly of pyrophosphates, short chains start to form at temperatures above 130 °C, which develop into longer polyphosphates close to 150 °C, which was attributed to be due to thermo-oxidative processes [2,21]. Thermal films were shown to reach a thickness of up to 400 nm [25] with an indentation modulus of 35 GPa and a hardness of 1.5 GPa [7], whereby no iron atoms are incorporated into the thermal films for iron-containing substrates [26]. Similar compositions occur for tribofilms, even though iron phosphates are found to form within the tribofilms for iron-containing substrates [26], whereby the mechanical properties are improved. In the synthesis process, blocks of zinc phosphate glass form and merge together, keeping their general shape. Film thicknesses of up to 150 nm can be reached [8]. While most of the film consists of ortho- and pyrophosphates, a top layer of longer polyphosphates can be found [2,7,21,27]. Ueda et al. [9] reported that the tribofilms can be amorphous at the surface and nanocrystalline at the interface to the substrate. This is in agreement with Nicholls et al., who showed that longer polyphosphate chains are present at the surface, while shorter chains were observed close to the substrate interface [28]. Zhang et al. reported that the tribofilm formation rate is dependent on the shear stress occurring during rubbing by reducing the thermal activation barrier for such film formation [24]. For

prolonged rubbing, the films become more nanocrystalline, whereby longer phosphate chains are broken into shorter ones, which was attributed to shear stress as well as heat arising during the rubbing process, increasing their wear resistance [9]. Additionally, a correlation between the morphology of the films and the chain length was demonstrated by Canning et al., whereby larger pads in the tribofilms correlate with longer polyphosphate chains, while smaller pads possess shorter polyphosphate chains [29]. The mechanical properties of tribofilms are characterized by a hardness of 3.5 GPa and a Young's modulus of 90 GPa [2] with a typical friction coefficient of 0.115 [30].

Heuberger et al. [16] investigated zinc phosphate films formed on hardened bearing steel (100Cr6), in a ball-on-disc tribometer, under mechanical pressure with 1 wt% ZDDP as an additive in poly-α-olefin (PAO). Hereby, a correlation between the applied pressure and the chain length as well as the thickness of the films was determined. The frictional heat generated under higher loads during the sliding process leads to longer chains and thicker films, which was attributed to thermal decomposition [21,27]. Similarly, an increase in temperature (up to 180 °C) results in longer chain lengths and thicker tribofilms [16]. The friction coefficients of these films vary between 0.14 at room temperature to 0.2 for higher temperatures (180 °C), whereby a linear dependence was observed. This increase in friction might originate from the higher chain lengths, but could also be based on the change in film thickness [16].

Dobbalaere et al. produced zinc phosphate thin films with plasma-enhanced atomic layer deposition that were P-rich with a P/Zn ratio of 2.3, therefore consisting of metaphosphate with some ultraphosphate contributions and a maximum reported thickness of <50 nm at a growth rate of 0.92 nm/cycle [31].

The wear resistance increase caused by ZDDP is generally attributed to the formation of phosphate-based tribolayers, hindering metal-to-metal contact in case of mixed or boundary lubrication spikes [23], which is supported by S-free zinc dialkylphosphates (ZP) possessing similar tribofilm thicknesses and wear behavior as ZDDP [32,33].

In contrast to the studies above, the goal of this work is therefore the direct synthesis of zinc phosphate glass coatings by magnetron sputtering and to demonstrate that the mechanical and wear properties can be controlled through intentional variation of the phosphate chain length. Hence, the synthesis of a sulfur-free tribolayer is demonstrated, providing an alternative model system to the ZDDP based, sulfur-containing tribolayers that need to be formed in the tribocontact.

To that end, magnetron sputtered zinc phosphate glass coatings were annealed, adjusting their composition and thereby their mechanical and wear properties, which is monitored by means of X-ray photoelectron spectroscopy (XPS), transmission electron microscopy (TEM), energy dispersive X-ray spectroscopy (EDX), nanoindentation and linear reciprocating wear testing.

2. Experimental details

Zinc phosphate glass coatings were synthesized by radio frequency magnetron sputtering of a $Zn_3(PO_4)_2$ target (American Elements) in a high-vacuum deposition chamber on 10×10 mm silicon substrates. The base pressure was below $3 \cdot 10^{-7}$ mbar and sputtering was conducted in argon (99.9999% Ar) at a pressure of 0.1 Pa with a power density of 3.45 W/cm². The deposition rate was approximately 500 nm/h at a source to substrate distance of 11 cm.

The as deposited samples were then annealed in ambient air in a GERO (SR70–200/12) tube furnace at temperatures between 100 and 400 °C in 50 °C increments. The samples were inserted into the furnace at the desired temperatures and removed after 3 h. Additionally, samples were annealed at 400 °C in a nitrogen and oxygen atmosphere for 1 h as well as under vacuum conditions for 10 min.

To analyze the chemical composition as well as the binding characteristics of 1 μm thick coatings, XPS was performed with a Kratos AXIS Supra (AL $K_α$ source: 1486.6 eV) and a pass energy of 10 eV. The

chemical composition was determined from overview scans using a dwell time of 99.5 ms and a step size of 1 eV. Characteristic ratios were analyzed with detail scans, whereby 10 sweeps, a dwell time of 300 ms and a step size of 0.1 eV were averaged. A Shirley background, a mixed Gaussian-Lorentzian peak shape (30–70%) and the relative sensitivity factors (RSF), provided by KRATOS, were considered. Peak calibration was performed for the C 1s peak with a binding energy of 284.8 eV.

The structures of the coatings were investigated in a Bruker AXS D8 Discover diffractometer, including a General Area Diffraction System (GADDS) using a copper target (Cu K$_\alpha$: λ = 1.5418 Å) with X-ray diffraction (XRD). Hereby, 2θ was varied between 30 and 90° with an accelerating voltage of 40 V and a current of 40 mA.

For the in-depth characterization, as well as the analysis over the whole coating thickness, STEM imaging and EDX mapping was conducted in a TEM Themis 200 G3 with a SuperX detector. A FEI Helios Nanolab 660 dual-beam microscope was used to prepare the TEM lamella by focused ion beam (FIB) milling with gallium ions and the subsequent milling to a thickness of around 80 nm.

To analyze the mechanical properties of the coatings, nano-indentation measurements were conducted with a Hysitron TI-900 TriboIndenter using the Oliver-Pharr method [34]. A fused silica standard was used to calculate the tip area function of the Berkovich diamond tip. With a load of 200 μN for the 5 × 5 indents per sample, a maximum contact depth of 35 nm for the coating thickness of ~2 μm was reached. Hence, the indentation depth corresponds to less than 2% of the film thickness and the influence of the substrate on the measured mechanical properties is therefore insignificant.

Wear resistance was investigated using a reciprocating linear tribometer Tetra Basalt MUST. The tests were done at room temperature with a 100Cr6 bearing steel ball with a 10 mm diameter as a counterpart under dry conditions as well as with a 9.65 mm diameter under poly-α-olefin (PAO) lubrication. Tests were repeated 3 times and performed at a sliding speed of 0.5 mm/s for 100 cycles, a stroke length of 1.5 and 3 mm and a load of 1 and 5 N, resulting in contact pressures of ~180 MPa and ~402 MPa for dry and lubricated conditions, respectively.

3. Results and discussion

### 3.1. Chemical analysis

Zinc phosphate glass coatings deposited from a $Zn_3(PO_4)_2$ target at room temperature possess an X-ray amorphous structure, see Supplementary Fig. S1. XPS analysis reveals a chemical composition of approximately 30 at.% Zn, 23 at.% P, 38 at.% O and 9 at.% C on the surface. Additionally, the ratio of the bridging (green curve) and non-bridging oxygen (red curve) peaks constituting the O 1s peak, was determined (see Fig. 1). According to Brow et al. [15] and Crobu et al. [17], the phosphate chain length can be determined based on the BO/NBO of the O 1s signal. As shown in Fig. 1, phosphate glass is composed of tetrahedral building blocks, where bridging oxygen, colored in green, is connecting the individual phosphate building blocks, which contain non-bridging oxygen, colored in red. Therefore, an increasing BO/NBO ratio corresponds to an increase in phosphate chain length, see Table 1 and Fig. 1. Hence, the shortest possible chain is characterized by the absence of bridging oxygen with a corresponding BO/NBO ratio of 0, see "orthophosphate" [16,17], Fig. 1. If two of the tetrahedral building blocks are connected via one bridging oxygen atom, the BO/NBO ratio of the so formed pyrophosphate is 1/6 [16,17], see "pyrophosphate", Fig. 1. The more tetrahedra are connected via bridging oxygen atoms, the longer the chains are, whereby chains within the BO/NBO ratio regime between 1/6 and 0.5 are characterized by chain lengths >2, see "polyphosphate", Fig. 1. Once all building blocks are connected (without cross-links), metaphosphate chains form with a BO/NBO ratio of 0.5, see "metaphosphate" [16,17], Fig. 1.

Considering the above discussion, a qualitative analysis of the XPS data of the surface shown in Fig. 1, indicates a decrease in chain length as the annealing temperature is increased. In Fig. 2, the BO/NBO ratio of the surface is plotted against the annealing temperature to enable a quantitative analysis of thermally induced changes in the phosphate chain length. In the as deposited state, metaphosphate chains seem to dominate, correlating to a BO/NBO ratio of 0.5 [16]. After annealing at
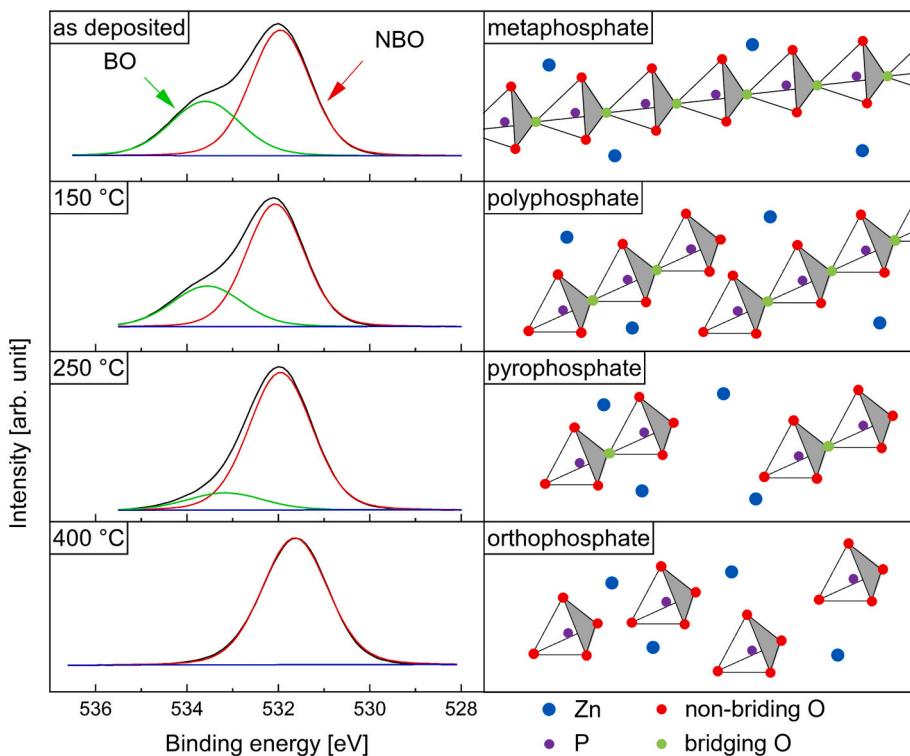
Fig. 1. XPS O 1s peak split into bridging (BO) and non-bridging oxygen (NBO) for meta-, poly-, pyro- and orthophosphate. With decreasing BO content, the chain length is decreased, which correlates with the annealing temperature [16]. Depictions of different chain types reconstructed after [17].
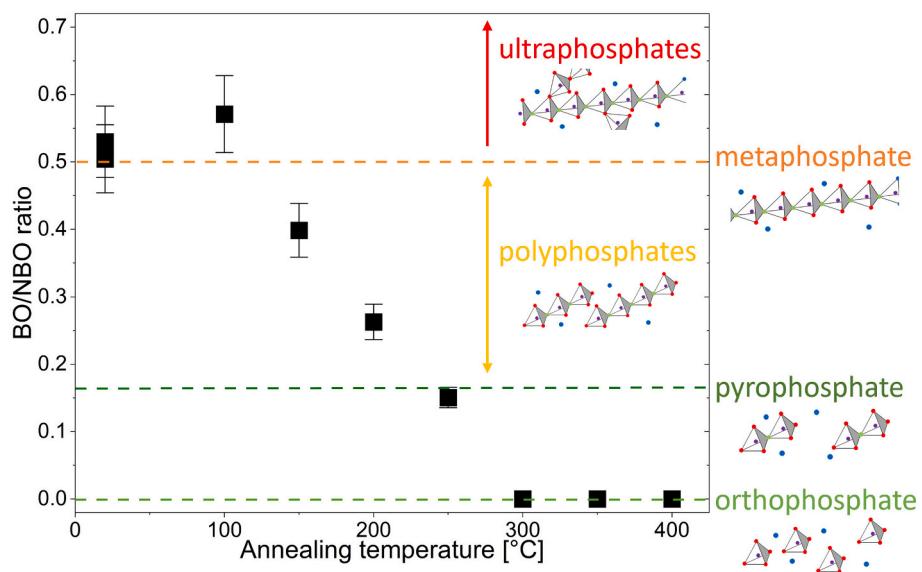
Fig. 2. Characteristic BO/NBO ratio obtained by XPS is used to determine the chain length. With increasing annealing temperature, a decrease in the chain length is observable. By sputtering and post-annealing, the same range of phosphates as reported by Heuberger et al. [16] can be achieved in a controlled manner with a linear decrease in chain length. Depiction of phosphate types modified after [17], classification into phosphate types based on BO/NBO ratios [16].

100 °C, metaphosphates that have started to cross-link (ultraphosphates), are present, while in the temperature region from 100 to 250 °C, the BO/NBO ratio decreases linearly from >0.5 to 1/6, implying a transition towards pyrophosphates [21]. After annealing in the temperature range of 300 to 400 °C, the formation of orthophosphates with a BO/NBO ratio of 0 is observed.

Heuberger et al. [16] investigated the formation of tribofilms in the tribological contact in the presence of ZDDP containing PAO lubricant at temperatures ranging from room temperature to 180 °C. The hereby obtained BO/NBO ratios were in the range of 0.1 to 1, indicating that tribofilms with similar chain lengths as obtained here are formed. Thereby, an initial alkylation of S in ZDDP is followed by a reaction of neighboring phosphoryl groups, which leads to the formation of longer poly- and cross-linked sulfur-containing phosphates [16]. In contrast, the here directly synthesized artificial sulfur-free, metaphosphate tribofilms can be transformed via thermally stimulated composition

changes into phosphates with shorter chains, ultimately resulting in the formation of orthophosphates.

Therefore, sputter deposition with subsequent annealing was successfully used to reach a similar coating composition and chain lengths as in sulfur-containing tribofilms, generated in a tribocontact of hardened bearing steel 100Cr6, when lubricated by a ZDDP containing oil [16]. Hence, artificial zinc phosphate coatings can be designed with a desired chain length.

To investigate, whether the composition alterations in the surface due to annealing, as probed by XPS, are also occurring in the bulk of the coating, EDX line scans were conducted in TEM for the as deposited sample, see also Supplementary Fig. S2, as well as for a sample after annealing at 400 °C. As can be seen in Fig. 3, a decrease in oxygen and phosphorus content relative to the zinc content can be observed over the whole thickness of the coating. This is in agreement with the XPS data and it can be concluded, that a homogeneous alteration of composition
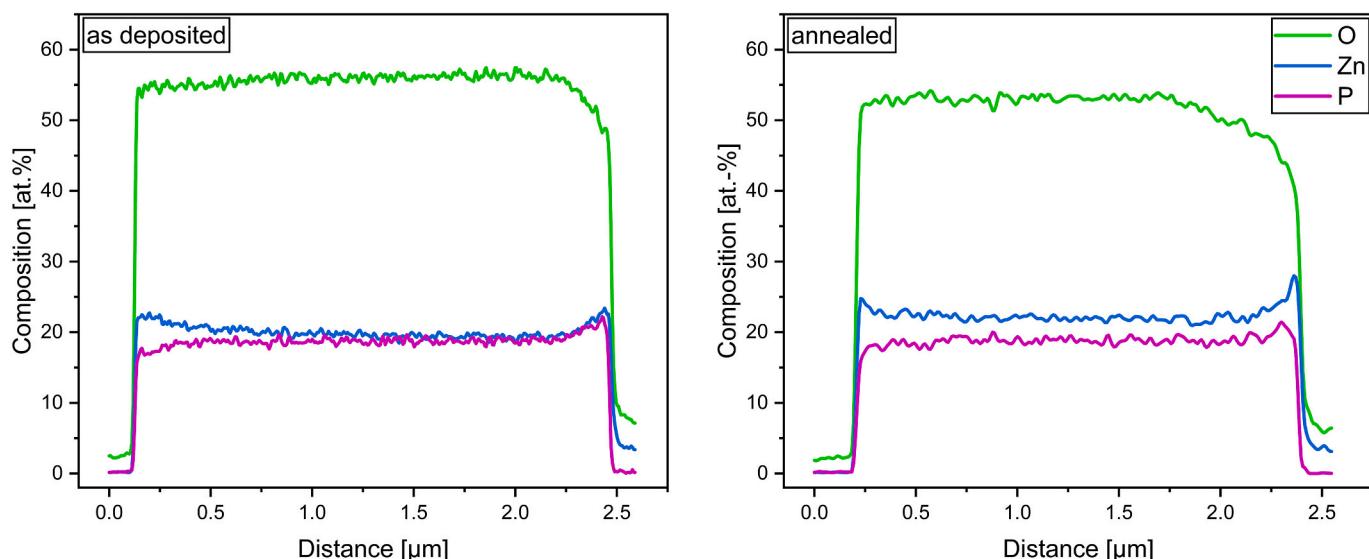
Fig. 3. TEM EDX linescan of as deposited sample and annealed at 400 °C for 3 h. The reduction of phosphorus in comparison to zinc is visible over the whole coating. Increased amounts of O and Zn for >2.5 μm can be explained by the presence of and interference with the protective Pt coating on top of the phosphate film, compare also Supplementary Fig. S2.

and, therefore, chain length over the whole coating was achieved with the above-described synthesis method.

3.2. Proposed mechanism

To gain a deeper understanding of the mechanism that leads to the formation of shorter chains, samples were annealed at 400 °C in different atmospheres in the XPS load-lock and analyzed directly with XPS. In Fig. 4 a), the BO/NBO ratios for coatings annealed in nitrogen, vacuum and oxygen are shown. While for all samples, a small decrease in BO/NBO and therefore a reduction in chain length is observable, the magnitude is significantly smaller than for samples annealed in air. This may be explained by the significantly smaller water partial pressure in nitrogen, vacuum and oxygen compared to ambient air, where the relative humidity was approximately 78% [35]. In both the XPS and EDX data, see Supplementary Fig. S3 and Fig. 3, a reduction of phosphorus and oxygen in relation to zinc was observable, with a P/Zn and O/Zn ratio of 0.79 and 1.28 for the as deposited coating, decreasing to 0.32 and 0.59 after annealing in ambient air at 400 °C, respectively. Zinc phosphate glasses are known to be prone to hydrolysis, whereby the phosphate chains, consistent with the observations reported here, are broken [36,37] via a reaction with water and by protonation, phosphoric acid is formed (see Fig. 4 b)) [38].

Thereby, water molecules diffuse into the bulk of the coating, initiating hydrolysis in addition to the surface [37]. Furthermore, the surplus of zinc, compared to the as deposited state, that is created during annealing amplifies the effect as zinc functions as a glass modifier, breaking up the chains via reactions with bridging oxygen [19].

### 3.3. Influence of chain length alteration on mechanical properties

To evaluate the influence of the chain length modification on the mechanical behavior, nanoindentation was performed using ~2 μm thick coatings and the annealing protocol from Fig. 2. Assuming that the annealing-induced changes in chain length are independent of coating thickness, hardness, see Fig. 5 a), and reduced Young's modulus values, see Fig. 5 b), were plotted versus the BO/NBO ratio determined for the 1 μm thick coatings discussed in Fig. 2. Fig. 5 a) shows the hardness as a function of the BO/NBO ratio. In general, a trend to lower hardness values for longer chain lengths can be observed. The hardness values

obtained for longer chains with BO/NBO ratios ranging from 0.57 to 0.26 are less than 4 GPa, similar to the reported hardness values of 3 and 4 GPa for ZDDP tribofilms with BO/NBO ratios of 0.54 and 0.27, respectively [39]. In contrast, coatings with shorter chain lengths possess hardness values of up to 5.5 GPa at a BO/NBO ratio of 0. A similar trend is visible in Fig. 5 b) for the reduced Young's modulus as a function of BO/NBO ratio, with an overall decrease in reduced Young's modulus from 84 to 65 GPa for longer chain lengths.

3.4. Wear and friction behavior

To probe the influence of the chain length on the tribological behavior, the as deposited coating as well as a sample annealed at 400 °C were analyzed in a reciprocating linear tribometer. The results shown in Fig. 6 a) demonstrate a comparable friction coefficient for the annealed and as-deposited sample of ~0.1 in a PAO lubrication environment. A steady state friction coefficient of ~0.12 was reached after 400 s of run-in, whereby the annealed sample exhibits with 0.017 a factor 6 lower initial friction coefficient than the as deposited coating. This might be due to differences in surface roughness of the annealed sample composed of orthophosphate as well as the higher hardness and reduced Young's modulus in comparison to the metaphosphate of the as deposited sample. The friction coefficients are comparable to tribofilms formed by ZDDP as reported by Heuberger et al. (between 0.14 and 0.2 for identical load and increasing temperature) [16]. The increase in friction coefficient for increasing temperatures in the case of Heuberger is most probably determined by larger film thicknesses and not due to the change in chain length.

The wear depths of the as deposited coating and the at 400 °C annealed sample are shown in Fig. 6 b). The maximal wear depth of the annealed sample is 54% smaller than the one measured for the as-deposited sample. Thereby, while the steady state friction coefficient is similar for both coatings, the post-deposition annealing treatment leads not only to a strongly reduced phosphate chain length, but also to a significantly increased wear resistance of the protective coating, reducing the wear volume of the as deposited sample of $3.0 \cdot 10^{14}$ nm^3 by factor 3.5 to a wear volume of $8.6 \cdot 10^{13}$ nm^3 for the annealed sample, correlating with the higher hardness and reduced Young's modulus for the annealed sample, see Fig. 5. The roughness of the side of the wear scratch can be explained by build-ups during the rubbing process. This is
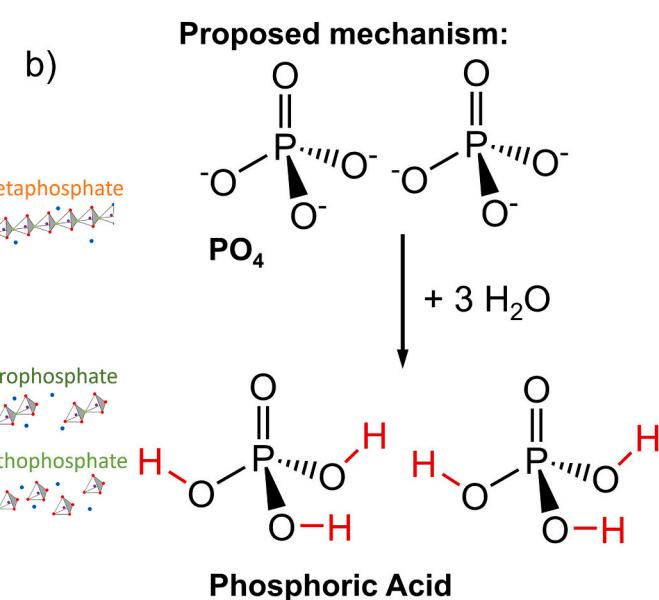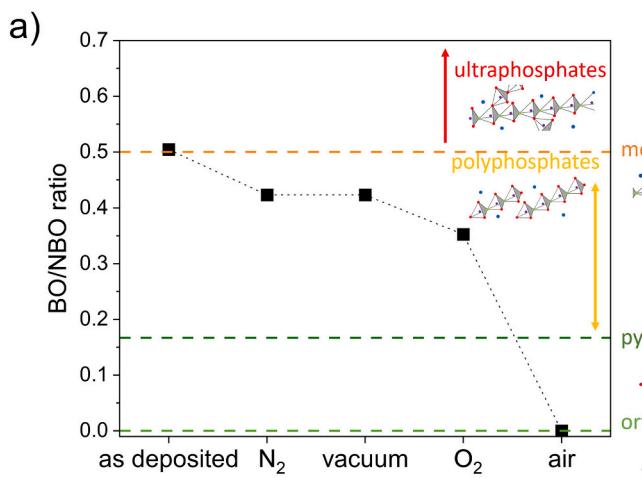
Fig. 4. a) BO/NBO ratio for samples annealed at 400 °C in nitrogen, vacuum and oxygen. All of them show a slight decrease in chain length, but not as pronounced as in air. The line connecting the datapoints is a guide to the eye. b) Proposed mechanism of hydrolysis due to the moisture in air is presented as a possible reason for this deviation.
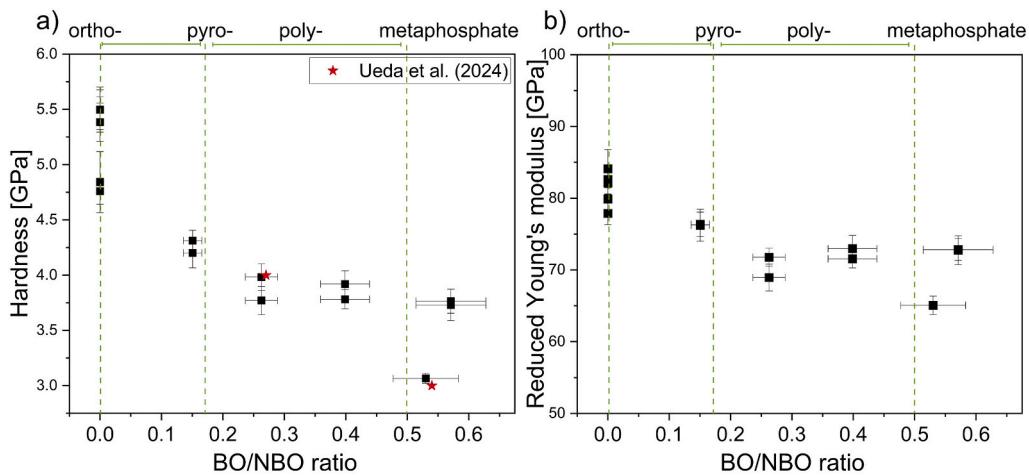
Fig. 5. Hardness and reduced Young's modulus for different chain lengths from annealed samples as well as hardness values for different BO/NBO ratios obtained from Ueda et al. [39] for tribofilms generated in a ball-and-disc tribometer on AISI52100 in a ZDDP solution. With decreasing chain length, both hardness and Young's modulus are increased up to the orthophosphate chain length. The hardness and reduced Young's modulus of the Si substrate were 12.18 ± 2.15 GPa and 145.12 ± 11.64 GPa, respectively.
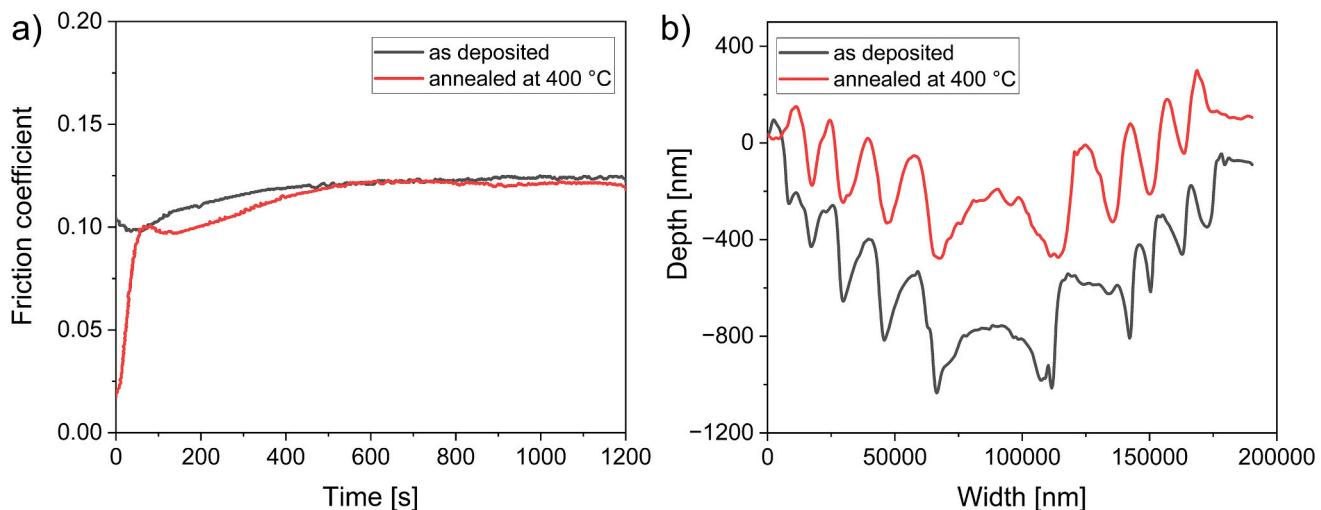
Fig. 6. Friction coefficient in PAO lubrication environment and wear track depths in dry environment after 100 cycles and a load of 5 N. Wear resistance of the annealed sample (400 °C) is increased in comparison to as deposited sample.

in agreement with Ueda et al. who reported an increased wear resistance for ZDDP tribofilms with shorter phosphate chains forming upon longer rubbing [9].

It is evident that annealing induced changes in chain length allow for the design of the mechanical properties and wear behavior of artificial zinc phosphate glass tribofilms. Such artificial tribofilms may prove useful in the investigation of long standing issues such as tribofilm replenishment and removal [23] for example via chemical state analysis of surfaces prior and after tribotesting within ZDDP-containing oil.

4. Summary

Annealing-induced composition modifications of magnetron sputtered sulfur-free zinc phosphate glass coatings were shown to systematically alter the chain lengths from meta- to orthophosphates, likely by hydrolysis with water in the atmosphere, enabling the controlled tailoring of mechanical properties. Thereby, artificial tribofilms with similar chain lengths as were obtained for sulfur-containing tribofilms, generated in a ZDDP-containing oil in a hardened bearing steel 100Cr6 tribocontact, were synthesized directly. Overall, the decrease in chain

length as probed by XPS can be attributed to a loss of phosphorus and oxygen upon annealing. Simultaneously, nanoindentation revealed that the change in chain length and composition linearly influenced the mechanical properties, increasing the hardness and reduced Young's modulus by 79% and 29%, respectively, providing a useful tool to design coatings with desired properties. Thereby, also the wear resistance for samples with shorter chain lengths is increased. In summary, artificial zinc phosphate glass tribofilms were synthesized that allow precise designing of the mechanical and wear properties to desired values by altering the chain length in a post-annealing treatment.

CRediT authorship contribution statement

Sebastian Lellig: Writing – review & editing, Writing – original draft, Visualization, Validation, Software, Methodology, Investigation, Formal analysis, Data curation, Conceptualization. **Subisha Balakumar:** Writing – review & editing, Validation, Investigation, Formal analysis. **Peter Schweizer:** Writing – review & editing, Visualization, Validation, Software, Investigation, Formal analysis. **Eva B. Mayer:** Writing – review & editing, Investigation, Formal analysis. **Simon**

Evertz: Writing – review & editing, Validation, Supervision, Conceptualization. **Marcus Hans:** Writing – review & editing, Validation, Investigation. **Damian M. Holzapfel:** Writing – review & editing, Validation, Investigation. **Yin Du:** Writing – review & editing, Validation, Investigation, Formal analysis. **Qing Zhou:** Writing – review & editing, Visualization, Validation, Resources, Methodology, Investigation, Formal analysis. **Martin Dienwiebel:** Writing – review & editing, Validation, Resources. **Johann Michler:** Writing – review & editing, Validation, Supervision, Resources, Project administration, Funding acquisition. **Jochen M. Schneider:** Writing – review & editing, Writing – original draft, Validation, Supervision, Project administration, Funding acquisition, Conceptualization.

Declaration of competing interest

The authors declare the following financial interests/personal relationships which may be considered as potential competing interests: Marcus Hans: Given his role as editor, Marcus Hans had no involvement in the peer review of this article and had no access to information regarding its peer review. Full responsibility for the editorial process for this article was delegated to another journal editor. Jochen M Schneider: Given his role as member of the editorial board, Jochen M Schneider had no involvement in the peer review of this article and had no access to information regarding its peer review. Full responsibility for the editorial process for this article was delegated to another journal editor. If there are other authors, they declare that they have no known competing financial interests or personal relationships that could have appeared to influence the work reported in this paper.

Acknowledgments

Appendix A. Supplementary data

Supplementary data to this article can be found online at https://doi.org/10.1016/j.surfcoat.2026.133181.

Data availability

Data will be made available on request.

References

[1] M. Awang, A.A. Khalili, S.R. Pedapati, A review: thin protective coating for wear protection in high-temperature application, Metals 10 (1) (2019) 42.
[2] H. Spikes, The history and mechanisms of ZDDP, Tribol. Lett. 17 (3) (2004) 469–489.
[3] H. Fujita, R. Glovnea, H. Spikes, Study of zinc dialkydithiophosphate antiwear film formation and removal processes, part I: experimental, Tribol. Trans. 48 (4) (2005) 558–566.
[4] L. Taylor, H. Spikes, Friction-enhancing properties of ZDDP antiwear additive: part I—friction and morphology of ZDDP reaction films, Tribol. Trans. 46 (3) (2003) 303–309.
[5] M.A. Nicholls, et al., Review of the lubrication of metallic surfaces by zinc dialkyl-dithiophosphates, Tribol. Int. 38 (1) (2005) 15–39.
[6] H. Fujita, H. Spikes, Study of zinc dialkyldithiophosphate antiwear film formation and removal processes, part II: kinetic model, Tribol. Trans. 48 (4) (2005) 567–575.
[7] M. Aktary, M.T. McDermott, G.A. McAlpine, Morphology and nanomechanical properties of ZDDP antiwear films as a function of tribological contact time, Tribol. Lett. 12 (2002) 155–162.
[8] J. Dawczyk, et al., Film thickness and friction of ZDDP tribofilms, Tribol. Lett. 67 (2) (2019) 34.
[9] M. Ueda, A. Kadiric, H. Spikes, On the crystallinity and durability of ZDDP tribofilm, Tribol. Lett. 67 (2019) 1–13.
[10] L.B. Fletcher, et al., Direct femtosecond laser waveguide writing inside zinc phosphate glass, Opt. Express 19 (9) (2011) 7929–7936.
[11] U. Caldiño, et al., New greenish-yellow and yellowish-green emitting glass phosphors: Tb3+/Eu3+ and Ce3+/Tb3+/Eu3+ in zinc phosphate glasses, J. Lumin. 135 (2013) 216–220.
[12] R. Martínez-Martínez, et al., White light generation through the zinc metaphosphate glass activated by Ce3+, Tb3+ and Mn2+ ions, JOL 129 (11) (2009) 1276–1280.
[13] L.Y. Niu, et al., A study and application of zinc phosphate coating on AZ91D magnesium alloy, Surf. Coat. Technol. 200 (9) (2006) 3021–3026.
[14] M. Sadeghi-Aghbash, M. Rahimnejad, Zinc phosphate nanoparticles: a review on physical, chemical, and biological synthesis and their applications, Curr. Pharm. Biotechnol. 23 (10) (2022) 1228–1244.
[15] R.K. Brow, The structure of simple phosphate glasses, J. Non-Cryst. Solids 263 (2000) 1–28.
[16] R. Heuberger, A. Rossi, N.D. Spencer, XPS study of the influence of temperature on ZnDTP tribofilm composition, Tribol. Lett. 25 (3) (2007) 185–196.
[17] M. Crobu, et al., Chain-length-identification strategy in zinc polyphosphate glasses by means of XPS and ToF-SIMS, Anal. Bioanal. Chem. 403 (5) (2012) 1415–1432.
[18] H. Liu, T. Chin, S. Yung, FTIR and XPS studies of low-melting PbO-ZnO-P2O2 glasses, Mater. Chem. Phys. 50 (1) (1997) 1–10.
[19] J.M. Martin, Antiwear mechanisms of zinc dithiophosphate: a chemical hardness approach, Tribol. Lett. 6 (1999) 1–8.
[20] G. Bancroft, et al., Mechanisms of tribochemical film formation: stabilityof tribo- and thermally-generated ZDDP films, Tribol. Lett. 3 (1) (1997) 47–51.
[21] R. Heuberger, A. Rossi, N.D. Spencer, Pressure dependence of ZnDTP tribochemical film formation: a combinatorial approach, Tribol. Lett. 28 (2) (2007) 209–222.
[22] L. Taylor, H. Spikes, Friction and wear behavior of zinc dialkyldithiophosphate additive, Tribol. Trans. 43 (3) (2000) 469–479.
[23] H. Spikes, Mechanisms of ZDDP—an update, Tribol. Lett. 73 (1) (2025) 38.
[24] J. Zhang, H. Spikes, On the mechanism of ZDDP antiwear film formation, Tribol. Lett. 63 (2) (2016) 24.
[25] M. Aktary, M.T. McDermott, J. Torkelson, Morphological evolution of films formed from thermooxidative decomposition of ZDDP, Wear 247 (2) (2001) 172–179.
[26] F.M. Piras, A. Rossi, N.D. Spencer, Combined in situ (ATR FT-IR) and ex situ (XPS) study of the ZnDTP-iron surface interaction, Tribol. Lett. 15 (2003) 181–191.
[27] Z. Yin, et al., Application of soft X-ray absorption spectroscopy in chemical characterization of antiwear films generated by ZDDP part I: the effects of physical parameters, Wear 202 (2) (1997) 172–191.
[28] M.A. Nicholls, et al., Chemomechanical properties of antiwear films using X-ray absorption microscopy and nanoindentation techniques, Tribol. Lett. 17 (2004) 245–259.
[29] G. Canning, et al., Spectromicroscopy of tribological films from engine oil additives. Part I. Films from ZDDP's, Tribol. Lett. 6 (3) (1999) 159–169.
[30] J. Zhang, et al., Boundary friction of ZDDP tribofilms, Tribol. Lett. 69 (2021) 1–17.
[31] T. Dobbelaere, et al., Plasma-enhanced atomic layer deposition of zinc phosphate, J. Non-Cryst. Solids 444 (2016) 43–48.
[32] K. Hoshino, et al., Tribological properties of sulphur-free antiwear additives zinc dialkylphosphates (ZDPs), SAE Int. J. Fuels Lubr. 5 (1) (2012) 504–510.
[33] P. Njiwa, et al., Zinc dialkyl phosphate (ZP) as an anti-wear additive: comparison with ZDDP, Tribol. Lett. 44 (1) (2011) 19–30.
[34] W.C. Oliver, G.M. Pharr, An improved technique for determining hardness and elastic modulus using load and displacement sensing indentation experiments, J. Mater. Res. 7 (6) (1992) 1564–1583.
[35] RWTH Aachen University Physikalisches Institut, A, Wetterstatistik Aachen 2020, 25.02.25, 11:25 am]; Available from: https://wetterstation.physik.rwth-aachen.de/statistik_2020.php, 2020.
[36] H. Takebe, Y. Baba, M. Kuwabara, Dissolution behavior of ZnO–P2O5 glasses in water, J. Non-Cryst. Solids 352 (28–29) (2006) 3088–3094.
[37] S.E. Ruiz-Hernandez, R.I. Ainsworth, N.H. de Leeuw, A molecular dynamics study of the effect of water diffusion into bio-active phosphate-based glass surfaces on their dissolution behaviour, J. Non-Cryst. Solids 548 (2020) 120332.
[38] B.S. Bae, M.C. Weinberg, Oxidation–reduction equilibrium in copper phosphate glass melted in air, J. Am. Ceram. Soc. 74 (12) (1991) 3039–3045.
[39] M. Ueda, H. Spikes, ZDDP tribofilm formation and removal, Tribol. Lett. 72 (4) (2024) 109.